

PAPER • OPEN ACCESS

## Mixed-valence hydrides at [FeFe]-hydrogenase active site mimics

To cite this article: Joseph A Wright *et al* 2023 *J. Phys.: Conf. Ser.* **2462** 012054

View the [article online](#) for updates and enhancements.

### You may also like

- [Gas-Diffusion and Direct Electron Transfer-Type Bioanode for Hydrogen Oxidation with Oxygen-Tolerant \[NiFe\]-Hydrogenase As an Electrocatalyst](#)  
Kenji Kano
- [Self-assembled supramolecular materials for photocatalytic H<sub>2</sub> production and CO<sub>2</sub> reduction](#)  
Jia Tian, Junlai Yu, Qingxuan Tang et al.
- [Electrocatalysis by Soluble \*Pyrococcus furiosus\* \[NiFe\]-Hydrogenase and its Hydrogenase Subcomplex: Tuning the Catalytic Bias](#)  
Anne Katherine Jones and Zahra Katherine Nazemi

# Mixed-valence hydrides at [FeFe]-hydrogenase active site mimics

Joseph A Wright<sup>\*,1</sup>, Atheer M Madlool<sup>1</sup> and Stephen P Cottrell<sup>2</sup>

<sup>1</sup> Energy Materials Laboratory, School of Chemistry, University of East Anglia, Norwich Research Park, Norwich NR4 7TJ, UK

<sup>2</sup> ISIS Facility, Rutherford Appleton Laboratory, Harwell Science Campus, Oxfordshire OX11 0QX, UK

E-mail: joseph.wright@uea.ac.uk

**Abstract.** The number of methods to study transient paramagnetic hydrides at organometallic centres is extremely limited. The reactivity of {2Fe2S} centres with protons to produce both diamagnetic and paramagnetic systems is of central interest in developing novel catalysts for hydrogen production, inspired by the [FeFe]-hydrogenase enzymes. Here, we show how a combination of spectroscopic and electrochemical techniques is allowing access to detail of the reactivity of key species on these pathways. Electron paramagnetic resonance and infra-red spectroelectrochemical approaches have been used to observe the reduction of pre-generated diamagnetic hydrides. In contrast, avoided level crossing muon spin resonance (ALC- $\mu$ SR) has been used to form the open-shell species directly and to examine the formation of short-lived intermediates in the reaction process. The combination of these techniques suggests the involvement of terminal hydrides or CO-protonation states on the pathway to the isolable bridging hydride products.

## 1. Introduction

Novel methods to produce dihydrogen in the absence of platinum-group metals are of vital importance on delivering a post-fossil fuel economy. Nature has solved this problem in metalloenzymes called hydrogenases [1–4]. In particular, the [FeFe]-hydrogenase enzymes have evolved to perform the very same task at rates that rival platinum electrodes [5]. Mimicking this reactivity in small synthetic models is vital if this extraordinary chemistry is to be exploited on a large scale: the oxygen-sensitivity, size and mass of the whole enzymes precludes their use in production-scale environments. Whilst there are many structural models available today, truly biomimetic reactivity is extremely rare [6, 7]. The development of more effective catalysts requires both synthetic effort and insight into the reactivity of the metal hydrides which are central to catalysis [8, 9].

Model (diamagnetic) {2Fe2S} clusters can be synthesised, with simple ‘hexacarbonyl’ systems (**1a** and **1b**) available in a single step from commercial material (Figure 1). Replacement of two CO ligands in these materials leads to the more electron-rich systems **2a** and **2b** containing phosphines, and the highly-reactive dicyanides **3a** and **3b** [10]. Whilst **1a** and **1b** cannot be protonated by standard mineral acids, **2a** and **2b** react smoothly with acid to give isolable bridging hydrides [11]. The same reactions are much less tractable for the dicyanides as the lone pair present on the nitrogen atoms is readily attached in solution.



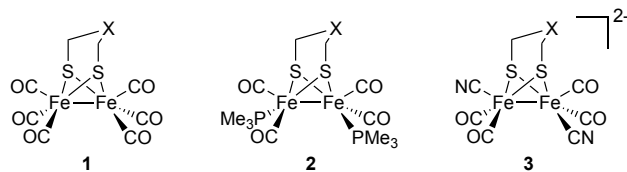


**Figure 1.** Model  $\{2\text{Fe}2\text{S}\}$  systems; X is empty for identifier **a** and is  $\text{CH}_2$  for identifier **b**

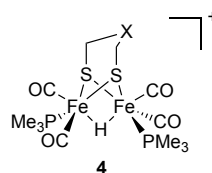


**Figure 2.** Isolable hydrides

Stopped-flow methods can be used to examine the formation of the bridging hydrides (**4a** and **4b**, Figure 2). On the seconds timescale, this technique demonstrates the involvement of several isomeric bridging hydrides on the pathway to the synthetically-isolable material [12]. Insight into the open-shell state of most direct relevance to catalysis is however lacking. Here, we provide a summary of our programme to study the Fe(I)–Fe(II) paramagnetic hydride state: it is this reactive hydride species which is central to the rapid turnover offered by the natural system [13, 14].

## 2. Reduction of pre-formed hydrides

### 2.1. Infra-red spectroelectrochemistry (IR-SEC)

Reduction of the pre-formed bridging hydrides **4** has been carried out electrochemically in a custom infra-red cell (Figure 3) [13]. The diamagnetic parent complex **4b** shows two bands in the carbonyl region of the infra-red window, at  $1989\text{ cm}^{-1}$  and  $2031\text{ cm}^{-1}$ . The presence of two bands reflects averaging of the bridging position in **4b** and solution-phase broadening of formally distinct bands.

Reduction to the mixed-valence state gives new peaks at  $1900\text{ cm}^{-1}$  and  $1948\text{ cm}^{-1}$ , with the retention of both the number of bands and the relative positions. This is consistent with the first-formed product comprising a mixed-valence state but with no significant change in the molecular geometry. This first-formed product has a lifetime of around 1.6 s as estimated by cyclic voltammetry: after this time, the bands seen in the infra-red change in both position and pattern, with at least three bands seen for the daughter product.

Species **4a** shows the same pattern of behaviour, but with a shorter lifetime for the first paramagnetic product: this degrades after around 400 ms. Both reduction products can be re-oxidised to recover the spectral features of the diamagnetic parents.

### 2.2. Electron paramagnetic resonance (EPR)

Electron paramagnetic resonance (EPR) can be used to observe the unpaired spin in paramagnetic species directly. In that sense, this is a more direct method for studying the open-shell hydrides than infra-red approaches. Chemical reduction of **4b** in a low-temperature solution allows access to the open-shell species (Figure 4) [13]. Simulation of this spectrum yields a  $g$ -factor of 2.0066 along with three clear hyperfine couplings: two with the phosphorus atoms ( $A_{\text{iso}} = -41.7\text{ MHz}$ ) and the bridging hydride ( $A_{\text{iso}} = -75.8\text{ MHz}$ ). The assignment of the hydride coupling was

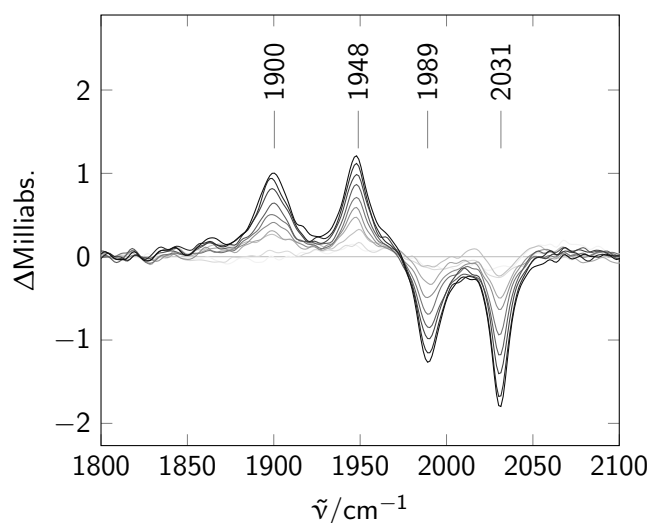


**Figure 3.** Infra-red spectrum showing the reduction of **4b** in tetrahydrofuran. Time scale 0.25 s (light grey) to 1.79 s (black), difference shown against a scan at 0.08 s. Modified from ref. [13]

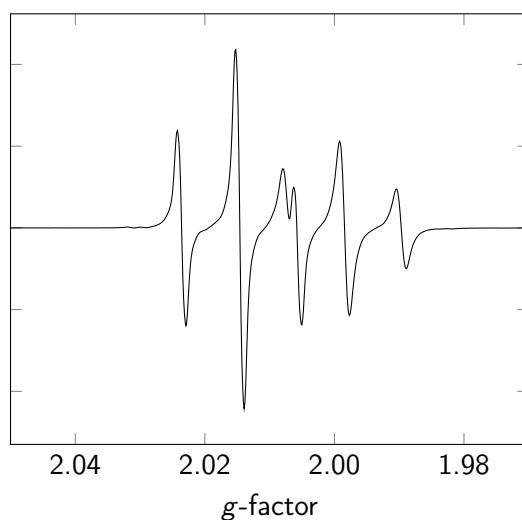


**Figure 4.** Continuous wave X-band EPR spectrum of **4b** reduced by acenaphthalene at 165 K in THF. Modified from ref. [13]

confirmed by synthesis of the equivalent bridging deuteride complex, which yields the anticipated 1 : 1 : 1 splitting and reduction in coupling constant.

### 2.3. Density function theory (DFT) simulation

Both the infra-red and EPR spectra for the open shell reduced **4b** were simulated using density functional theory (DFT) methods [13]. The changes seen in the infra-red spectra were supported by the computational data, with the movement of peaks of around  $90\text{ cm}^{-1}$  seen in both the experimental results and DFT simulations.

The two iron atoms bear a total of 70 % of the un-paired electron density. Approximately 3 % of the calculated spin density is located on the bridging hydride, while the two phosphorus atoms bear a total of 0.5 %.

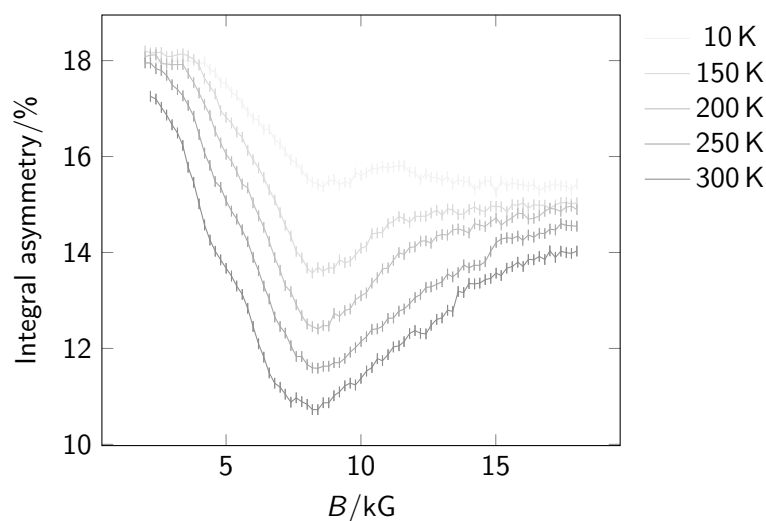


**Figure 5.** Time-integral ALC- $\mu$ SR spectra for **2b**. Data points are shown as sticks representing the estimated uncertainty in each point Modified from ref. [14].

hyperfine coupling values, the coupling constants obtained were in accord with those from the low-temperature experiments.

### 3. Avoided level crossing muon spin resonance (ALC- $\mu$ SR)

Central to the hydrogen chemistry carried out by the subsite is its interaction with protons. The data reported above allowed examination of the paramagnetic states at timescales down to as low as one second. However, much of the most interesting behaviour of these models occurs on much shorter timescale. For example, the location of the primary protonation sites is still an open question, with terminal and bridging hydrides possible candidates along with the sulphur, carbonyl and cyanide ligands. At the same time, the need to pre-form diamagnetic hydrides before reduction is a limiting factor in probing truly catalytic pathways.

Muonium, as a ‘light’ analogue of  $H^+$ , offers the means of studying the structure and dynamics of such chemistry on the nanosecond timescale. In particular, it offers the potential to access short-lived species which cannot be generated by reduction of pre-formed closed-shell precursors. This is particularly attractive in the search for transient hydride, as there are few alternative approaches, and none offering the selectivity and timeframe of muon methods.

Avoided level crossing muon spin resonance (ALC- $\mu$ SR) is a longitudinal field technique in which reduction in polarisation at ‘avoided’ cross-points in the Breit–Rabi diagram is probed. This method is conveniently available using the HiFi instrument at ISIS-RAL [15], offering a maximum applied field of 5 T: this is typically well in excess of the expected resonance position for molecular systems.

Complexes **1b**, **2b** and **3b** have been studied by ALC- $\mu$ SR [14], with all three compounds exhibiting a strong but extremely broad resonance centred around approximately 8 kG (Figure 5). All of these show a strong temperature-dependence, with the most prominent signal occurring at room temperature. In the case of **2b**, as well as the major resonance, a ‘shoulder’ could be seen at around 5 kG in the 300 K scan, which was lost as the temperature decreased (Figure 6). This small signal was absent in the spectra for **1b** and **3b**.

DFT simulation of a large number of potential addition sites was undertaken using the Gaussian 09 software package [16]. For all three complexes, the product structures in which muonium is bound into the Fe–Fe bridging site were found to give hyperfine couple constants

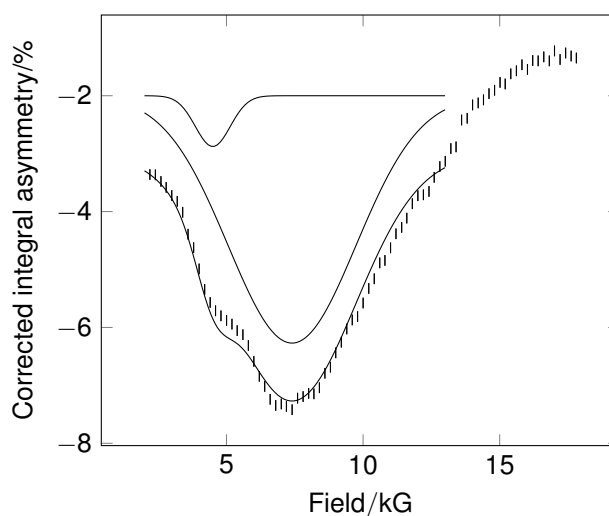


**Figure 6.** Background-subtracted time-integral ALC- $\mu$ SR spectra for **2b** at 300 K showing Gaussian line shape approximation for the range 2 kG to 13 kG. Reproduced from ref. [14].

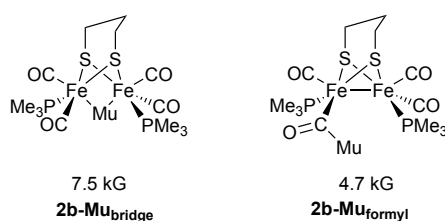


**Figure 7.** Potential sites of muon addition, and calculated resonance field values

consistent with the experimental data. Moreover, this was the only binding position which was common to all three substrates *and* gave an appropriate resonance position. Notably, these product structures can be regarded as isotopomers of the Fe(I)–Fe(II) bridging hydrides, *e.g.* the species obtained by one-electron reduction of **4b**.

In the phosphine complex **2b**, only one putative structure gave a hyperfine coupling which could account for the shoulder seen at around 5 kG: binding to a C=O to give a formyl-type radical (Figure 7). Species of this form have previously been suggested as one possible intermediate on the pathway to protonation of the metal–metal bond [17], and this experiment is thus the first experimental evidence for such an intermediate. No similar shoulder was observed in the spectra for **2a** or **2c**; this may reflect a difference in the timeframe for transfer of the bound muon from the carbonyl group in the three systems.

The reduction in intensity of the major resonance peak with decreasing temperature makes it possible to extract kinetic parameters for the muonation. The estimated activation energies rise from 1.58(3) kJ mol<sup>-1</sup> for **3b** to 3.40(2) kJ mol<sup>-1</sup> for **1b**. This order mirrors the reactivity of these systems toward protons, as detailed above.

Whilst structures containing a three-carbon bridge offer the greater similarity to the natural system, those with only two carbons between the sulphur atoms have higher symmetry. ALC data have been obtained at ISIS-RAL for **1a–3a**. DFT simulation of these systems is ongoing, and will allow a full analysis of this data to be presented in due course.

#### 4. Conclusions and outlook

A combination of approaches has been used to study paramagnetic hydrides at {2Fe2S} centres. Reduction of isolable closed-shell hydrides allows access to short-lived paramagnetic species in the chemistry laboratory. A combination of rapid infra-red and low-temperature EPR methods has established that on the second timescale, the first-formed paramagnetic bridging hydrides decompose to daughter products of lower symmetry. ALC- $\mu$ SR has been used to probe the direct formation of paramagnetic hydrides at short times, and gives evidence for both bridging muonides and formyl-like species.

#### Acknowledgments

The authors thank the Leverhulme Trust for funding (grant RPG-2019-115).

#### References

- [1] Tard C and Pickett C J 2009 *Chem. Rev.* **109** 2245–2274
- [2] Gloaguen F and Rauchfuss T B 2009 *Chem. Soc. Rev.* **38** 100–108
- [3] Simmons T R, Berggren G, Bacchi M, Fontecave M and Artero V 2014 *Coord. Chem. Rev.* **270–271** 127–150
- [4] Lubitz W, Ogata H, Rüdiger O and Reijerse E 2014 *Chem. Rev.* **114** 4081–4148
- [5] Frey M 2002 *ChemBioChem* **3** 153–160
- [6] Camara J M and Rauchfuss T B 2011 *Nat. Chem.* **4** 26–30
- [7] Wang N, Wang M, Wang Y, Zheng D, Han H, Ahlquist M S G and Sun L 2013 *J. Am. Chem. Soc.* **135** 1688–13691
- [8] Wright J A and Pickett C J 2014 Mechanistic aspects of biological hydrogen evolution and uptake *Bioinspired Catalysis* ed Weigand W and Schollhammer P (Wiley-VCH) pp 161–198 ISBN 978-3-527-33308-0
- [9] Schilter D, Camara J M, Huynh M T, Hammes-Schiffer S and Rauchfuss T B 2016 *Chem. Rev.* **116** 8693–8749
- [10] Lyon E J, Georgakaki I P, Reibenspies J H and Darensbourg M Y 1999 *Angew. Chem. Int. Ed.* **38** 3178–3180
- [11] Zhao X, Georgakaki I P, Miller M L, Yarbrough J C and Darensbourg M Y 2001 *J. Am. Chem. Soc.* **123** 9710–9711
- [12] Wright J A and Pickett C J 2009 *Chem. Commun.* **45** 5719–5721
- [13] Jablonskytė A, Wright J A, Fairhurst S A, Peck J N T, Ibrahim S K, Oganessian V S and Pickett C J 2011 *J. Am. Chem. Soc.* **133** 18606–18609
- [14] Wright J A, Peck J N T, Cottrell S P, Jablonskytė A, Oganessian V S, Pickett C J and Jayasooriya U A 2016 *Angew. Chem. Int. Ed.* **55** 14580–14583
- [15] Lord J S, McKenzie I, Baker P J, Blundell S J, Cottrell S P, Giblin S R, Good J, Hillier A D, Holsman B H, King P J C, Lancaster T, Mitchell R, Nightingale J B, Owczarkowski M, Poli S, Pratt F L, Rhodes N J, Scheuermann R and Salman Z 2011 *Rev. Sci. Instrum.* **82** 073904
- [16] Frisch M J *et al.* 2009 *Gaussian 09 Revision C.01* Gaussian Inc. Wallingford, CT, USA
- [17] Liu C, Peck J N T, Wright J A, Pickett C J and Hall M B 2011 *Eur. J. Inorg. Chem.* 1080–1093